FLOW PATTERNS AND THE IMPACT OF ACTIVE CHILLED BEAM LOCATION ON THERMAL COMFORT IN COMMERCIAL BUILDINGS

Abstract

Chilled beams are increasingly becoming popular as a means of heating and cooling in buildings, especially in the developed nations in Europe and the US, thanks to their low operating costs and better avenues for energy savings. Considering the fact that they are installed on the ceiling and functionally vent out air at an angle to the plane of the ceiling, there is a high likelihood of a strong interaction of the jet of air with either the boundaries of the room or objects within the room. These interactions lead to interesting patterns of air movement within the building space and are also essential in normalizing the effects of the outdoor extreme climatic conditions in case of the presence of an external window. In this work, we study the effects of such interactions on the air movements in the building space and, thereby, the impact it has on comfort conditions. With the premise that such interactions are important in achieving human thermal comfort, the location of the chilled beam on the ceiling is an interesting variable to optimize and investigate. Through a series of Computational Fluid Dynamic (CFD) simulations using ANSYS Fluent and Airpak software, we investigate the dynamics of interaction between airflows and thermal comfort of humans (using Fanger's Predictive Mean Vote, PMV, model) under the influence of an active chilled beam. These test cases from the CFD simulations are tested and validated against an experimental room set up in Andover, Massachusetts.

Authors

Nikhilesh Ghanta, Barry Coflan, and Leon Glicksman
Massachusetts Institute of Technology

Keywords

Chilled beams, thermal comfort, CFD

Nomenclature

T	Temperature	σ	Stephan-Boltzmann constant
q	Heat or Energy	e	Emissivity
H	Metabolic Heat Production	F	Area parameter
Pa	Vapor Pressure of Water Vapor		Density
Fcl	Clothing insulation parameter	U	Velocity Vector
P	Pressure	g	Acceleration due to gravity
Tcl	Clothing surface temperature		Dynamic viscosity
Tr	Mean radiant temperature	c	Specific heat capacity
Hc	Convective heat transfer coefficient	k	Thermal conductivity
Ta	Air temperature		

Introduction

Chilled beams are an increasingly popular choice of air conditioning equipment, primarily in the western world. A study by Future Market Insights in 2017 indicated that the value of the chilled beam market would rise by 120% in a span of 10 years, with a significant continuous annual growth rate of 6.4%. Although the primary market is the Western European region, the US is progressively increasing its chilled beam usage. The primary reason behind this increased interest in the chilled beams is its scope for being an energy efficient system, to provide better humidity and noise control with lower operating costs. Increasing risks of climate change have brought about stringent building energy codes in the developed nations in the US and Europe, and chilled beams provide a good alternative to conventional HVAC (Heating Ventilation and Air Conditioning) systems as a low energy comfort conditioning system. Although chilled beams demand higher installation costs, the return on investment is quite fast when designed properly and this is where the study of design parameters of chilled beam systems help.

Chilled beams usually are of two types—active and passive. Active chilled beams utilize the principle of induction to suck in air from the space onto the heat exchanging coil, as the primary air moves through the nozzles. This results in a higher cooling capacity than the passive chilled beam, which involves space air movement from the room onto the heat exchanging coils without any induction. Chilled beams also come in two varieties, like the fan coil units—4-pipe for both heating and cooling and 2-pipe for either cooling or heating alone. Multiple studies have been undertaken on the utility of active and passive chilled beams and their impact on the comfort levels of humans in the occupied zones. It is crucial to understand the interaction of jet flows from the chilled beams with the buoyant plumes from the heat sources in the room. This becomes even more important with solar loading in the room through external windows. The air flow pattern determines how quickly the conditioning happens in the room (Muller et al., 2004) and the external weather conditions play a major role in this interaction. These flow patterns and interactions were studied by Koskela et al. (2012) for the case of space cooling. This study aims at examining these interactions and their influence on human thermal comfort and thermal stratification in the room during various extreme outdoor climatic conditions and their corresponding indoor chilled beam conditioning—both cooling and heating.

The current study involves an active chilled beam with a 4-pipe connection, located in a commercial conference room in the heating dominated climate of Andover, Massachusetts, USA. This manuscript is based on experiments conducted in the room and computational simulations performed using ANSYS Fluent and Airpak. The impact of varying location of the chilled beam on the thermal comfort and stratification is also studied through simulations and airflow pattern through the door analyzed.

Methodology

A conference room in a commercial office space was chosen for the studies. The room has floor dimensions of 5.8mx5.5m and has a ceiling-floor distance of 2.8m. It has one side of the longer dimension as an external wall, facing north. The external wall has a large window, completely covering the entire wall area from a height of 0.75m until the ceiling. The other three walls are internal walls connected to other rooms of the building. The room has a false ceiling alongside the chilled beam ducts, rendering almost zero heat transfer through the top boundary of the room. The floor is concrete-based and acts as a thermal mass. The chilled beam is located 1m away from the external window and parallel to it and is 2.8m in length. The wall opposite the external window has a door with a leakage area around it. The door is 0.8m wide and 2.5m tall. The room has a projector connected to the ceiling and a couple of tables with multiple chairs, providing occupancy for a maximum of eight people to sit. Apart from the incoming solar radiation through the external window, the other sources of heat generation are the projector, humans, and laptops. Lighting used in the room is almost zero due to the large unshaded external window. Depending on the temperature set-point in the thermostat located on the wall opposite the external window, the chilled beam either cools or heats the space.

Experiments were conducted in the months of April and May, during which the outdoor temperature in Andover, Massachusetts, was in the range of 12°C–20°C. The measurements of velocity were conducted using hot-wire anemometers (TSI VelociCalc Air Velocity Meter 8345; +-0.015m/s accurate). Temperature readings at various locations in the interior room space were recorded using multiple thermocouples (TSI VelociCalc 8345; 0.3°C accurate), and surface temperatures were measured using an Infrared Camera (Flir E5 WiFi Infrared Camera; +-2% accurate), as shown in Figure 1. Additionally, the concentration of carbon dioxide in the room was also monitored (Telaire 7001 CO_2 sensor; +-50 ppm accurate). This is crucial in the operation of the active chilled beam with a control logic to bring in the outdoor fresh air to meet a specified setpoint of CO_2 concentration. This in effect would add additional conditioning load to the chilled beam.

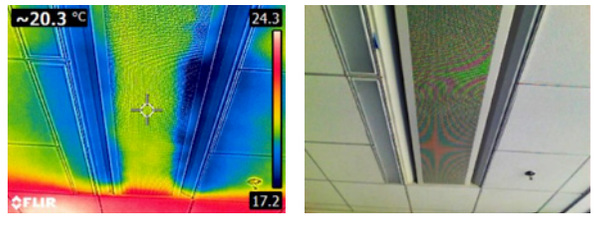

Figure 1: Sample snapshots of surface temperature measurements using Flir Infrared Camera in the test room.

One of the most widely used comfort calculation and analysis model for mechanical conditioning scenarios is the Fanger's PMV (Predictive Mean Vote) model. Fanger's PMV correlation is based on the identification of sweating rate and skin temperature needed for the optimal thermal conditions. A plausible set of equations to determine them are shown below (Equations 1 and 2), extracted from the data of Rohles and Nevins (1971).

Equation 1:

$$T_{sk,\,req} = 96.3 - 0.156 * q_{met,\,heat}$$

Equation 2:

$$q_{sweat,\,req} = 0.42 * (q_{met,\,heat} - 18.43)$$

PMV is calculated using the below set of equations (Equation 3).

Equation 3:

PMV = 4 + (0.303 exp(-0.036H) + 0.0275) x {6.57 + 0.46H + 0.31Pa + 0.0017H*Pa + 0.0014H*Ta - 4.13 fcl (1 + 0.01dT) (Tcl - Tr) – hc*fcl (Tcl - Ta)};

Where each individual variable term has its own separate equation based on the surrounding conditions of temperature, humidity, pressure, etc.

PMV is measured on a scale of -3 to 3, positive numbers indicating hot conditions and negative indicating cold. A higher magnitude of the PMV value indicates that the condition is more uncomfortable. Ideally, a range of +0.5 to -0.5 is considered a well-conditioned space for humans to occupy.

CFD Modeling

The room was modeled in Airpak and ANSYS to the exact scale, replicating most of the features of the room. Computational Fluid Dynamics (CFD) was used to simulate the room conditioning process. The chilled beam was approximately modeled using the exhaust and intake vents, with the inlet boundary conditions primarily taken from the manufacturer information and refined using experimental data collected for the outlet vent velocity. The two chilled beam outlet vents are located on either side of the inlet vent, with the air ducts allowing the air to enter the room at an angle. Air velocity recorded at this exhaust vent is measured along the flow direction. The inlet vent of the chilled beam takes in air vertically upward through a series of small ducts, arranged in a rectangular grid. The k-epsilon turbulent model was used for simulating the air flows. Radiation modeling was enabled through the surface to surface radiation, with the heat transfer rate defined as Equation 4.

Equation 4:

$$q = \sigma e F (T_{surface}^4 - T_{remote}^4)$$

Outdoor weather conditions were simulated using the epw file data obtained from the local Boston weather station. Adiabatic boundary conditions were imposed on all the internal walls, and the external wall was connected to the data from the epw file. All the heat sources were appropriately modeled with a specific heat flux emission as the boundary condition. The corridor connected through the door was assumed to be maintained at a relatively uniform temperature and was modeled as a significantly large area to avoid any end effects of the flow through the door. The floor was modeled as a finite thickness concrete slab, capable of acting as a thermal mass. Mesh refinement was applied to internal surfaces to appropriately account for the turbulence and boundary layers. The basic governing equations involved in the simulations using the finite volume method are the continuity equations and the conservation of momentum and energy. The actual compressible version of these equations used is shown below (Equations 5–7).

Equation 5:

$$\frac{\partial_\rho}{\partial_t} + \nabla.(\rho U) = 0$$

Equation 6:

$$\frac{\partial_{(\rho U)}}{\partial_t} + \nabla.(U.\rho U) - \rho g = -\nabla p. + \nabla.[\mu(\nabla U + (\nabla U^T)] - F_5$$

Equation 7:

$$\frac{\partial_{\rho c T}}{\partial_t} + \nabla.(U.\rho c U T) = \nabla.(k \nabla T + P \nabla.V$$

Where is the surface tension force at the interface, given by:

$$F_s = \frac{2_{\rho \delta_s}}{\rho_a + \rho_t} [\sigma k n]$$

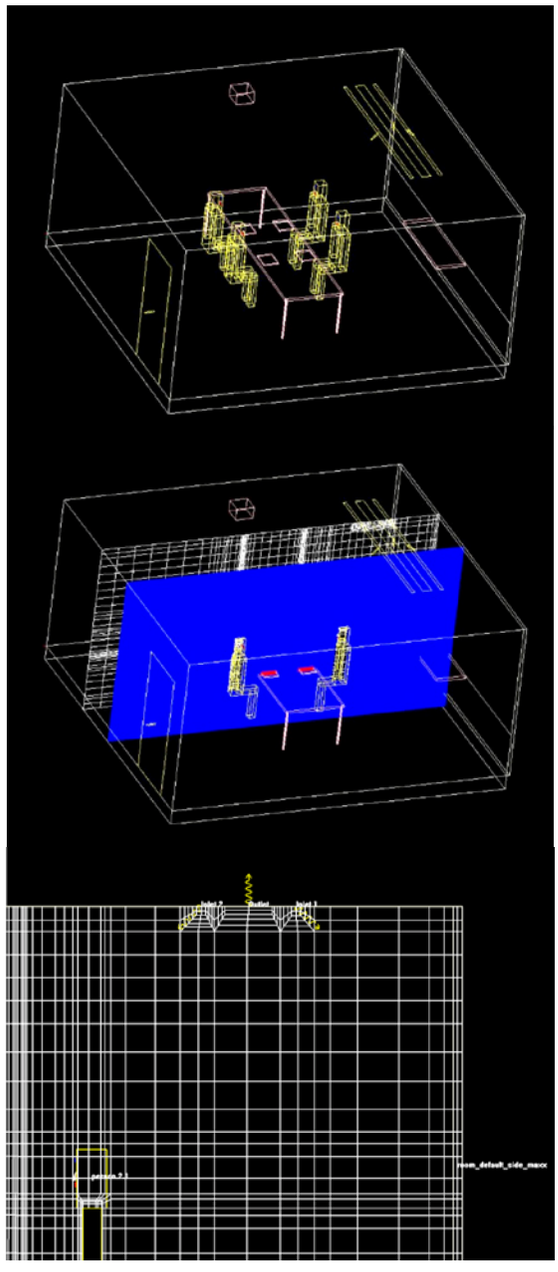

Figure 2: Modeled 3D geometry of the test room in ANSYS and Airpak (top); 3D model showing the two planes for post-processing–plane 1 in white checks and plane 2 in shaded color (middle); meshing of CFD near the chilled beam outlets and inlets (bottom).

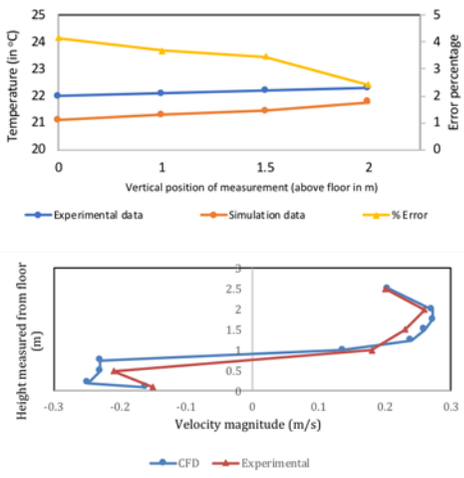

Figure 3: Validation plot for vertical distribution of temperature readings (top) and velocity readings (bottom) from experiments and CFD simulations with the door open; plotted with the error percentage.

The results of the CFD simulations were realized on the two planes as shown in Figure 2. These planes pass through the humans in the room and are perpendicular to the direction of the external wall. For the purposes of validation with experimental readings, the simulations performed considered four humans sitting in the room—two on each side of the center table. Grid independence study was performed with decreasing mesh size, especially near the internal surfaces where eddy flows and turbulence are prone to occur. A nominal value of mesh size was chosen where the change in accuracy of the simulated values of temperature and velocity were found to be less than 1% when doubling the number of grid points. A sample meshing of the grid is shown in Figure 2, around the inlet and outlet areas of the chilled beams. A total of 1,103,412 nodal points are considered in the mesh, with dynamic spacing.

A qualitative and quantitative validation study was performed with the experimental readings of temperature and velocity inside various locations of the room. The vertical gradient of temperature was also checked for in the accuracy of the numerical simulations. Figure 3 shows the comparative temperature and velocity readings from experiments and CFD simulations adjacent to the door, with the door being kept open. The CFD simulations gave reasonably accurate values and trends of temperature and velocities observed in the test room, keeping the error percentage within 5%–10%.

Results and Discussion

As observed by Koskela et al. (2012), the heat sources in the room showed a significant impact on the airflow pattern and thereby the temperature distribution in the room as well. The risk of a draft is usually attributed to the downfall of inlet jets and large-scale circulations. Along with these factors, the following factors were also identified through the simulation results of the work presented:

- The air circulation through an open door leading into the corridor.
- Presence of furniture (here, a table) in the room.

It was observed through the CFD simulation results that there is a directional change in the flow of air through the door as you move from the top of the door to the bottom. Somewhere around the middle of the door, there is a plane of zero velocity—a neutral plane. In specific cases of reduced flow into the chilled beam, two neutral planes are observed along the cross-section of the door. It is observed that the flow is mostly directed inward from the bottom half of the door, with the condition that the outdoor corridor is maintained at a relatively uniform temperature as compared to the room in consideration. This was also validated using a smoke pen experiment in the room, photographs attached in Figure 4. This clearly induces a significant amount of draft at the person sitting right by the door. During the summer and shoulder seasons when the conditioning required in the room is air cooling, there would be another complimentary yet directionally opposite airflow stream from the chilled beam onto the external window, leading finally toward the human sitting in front of the door. This would make that specific person in the room vulnerable to being uncomfortable. Figure 5 shows the velocity magnitude and distribution in the room, realized on plane 2. This shows the relative difference in magnitudes of the air velocities through the door and around other heat sources in the room. They are comparable in magnitude and can all contribute to draft within the room.

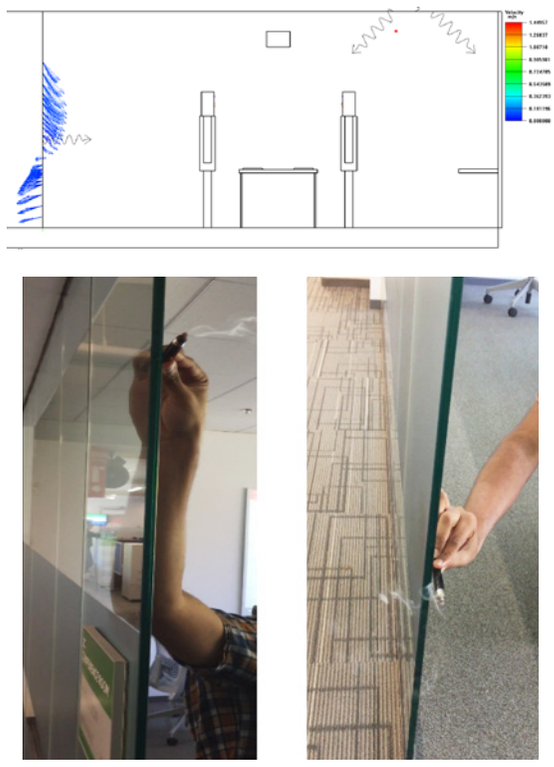

Figure 4: CFD Simulation results showing the air velocity and movement across the door (top); snapshots of experiments using smoke pen for determining qualitatively the airflow across the door (bottom).

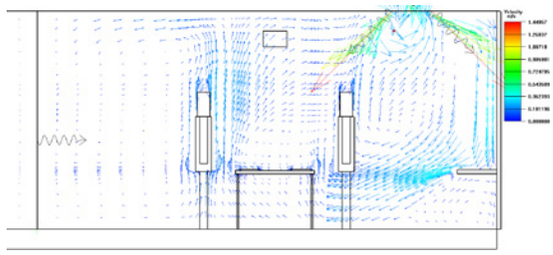

Figure 5: Velocity vectors plotted on plane 2 for the case of a cooling scenario in the summertime, showing the air flows and circulations.

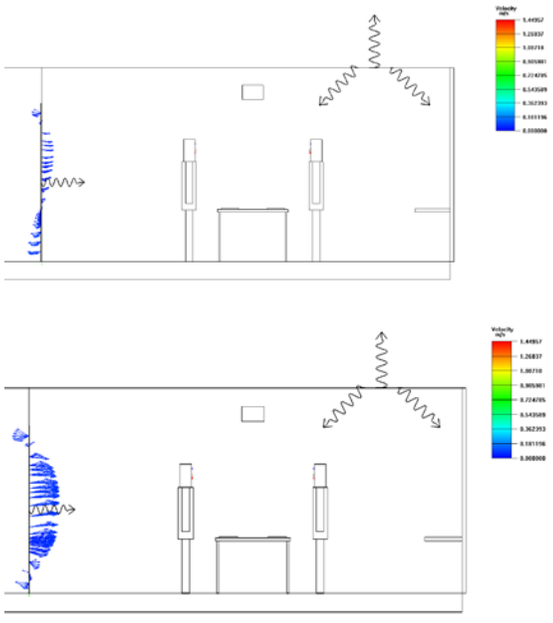

Figure 6: Sample simulation results of varying flow rate from the chilled beam to show the air flow pattern through the door—low chilled beam outlet velocity ~0.2m/s (top) and high chilled beam outlet velocity ~0.9m/s (bottom).

Figure 6 shows the direction and magnitude of air velocity through the open door, for multiple cases of varying airflow rate from the chilled beam. As can be seen from the simulation result snapshots, the flow through the door is certainly not uniform and varies both in magnitude and direction with the cooling capacity of the chilled beam. This also has an impact on the draft experienced by the persons sitting close to the open door. However, for the sake of analysis in this work, we maintained a single value for the airflow rate from the chilled beam.

A series of CFD simulations were run with a hypothetically varying location of the chilled beam on the ceiling. Three locations of the chilled beam were chosen for the simulations. The simulations were performed for varying seasons with each different location, to understand the impact of the placement of the chilled beam in effectively regulating the indoor conditions. Along with a vertical stratification of temperature, a horizontal stratification was also observed across the room, with the stratification intensity increasing as the chilled beam was moved away from the external window. It is clearly observed through the extreme temperature scenarios that the indoor conditioning is at its best when the chilled beam is closer to the external window. This strategic placement has a moderating effect of the presence of the external window and the effect of the outdoor conditions. Figures 7 and 8 show the temperature distribution on planes 1 and 2 respectively with different locations of the chilled beam for an outdoor ambient temperature of 35°C. This is on average the higher end of the temperature conditions for a place like Andover, Massachusetts.

The temperature of the incoming air into the test room from the chilled beam is 20°C. The scale of the temperature legend was set in order to observe its variation clearly. It is quite evident that as the chilled beam is located away from the external window, the influence of the external temperature on the indoor conditions is higher. This effect is very prominent on the person sitting closest to the external window. However, as the chilled beam is located just adjacent to the external window, one half of the jet emanating from the chilled beam falls along the window, thereby neutralizing the effects of the external extreme conditions and the other half is noticeably cooling the interior of the room, while interacting with the hot buoyant plumes from the heat sources. A similar observation can also be made from the case of the chilled beam located in the middle of the room, with a slight variation in the internal temperature from the case of the chilled beam on the right. A similar trend is observed for both the planes in consideration.

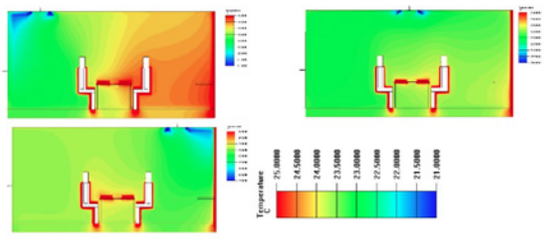

Figure 7: Temperature contours for an outdoor external temperature of 35°C, realized on plane 1 with varying positions of the chilled beam away from the external window (top left), middle of the room (top right), and next to the external window (bottom left); temperature legend is shown at the bottom.

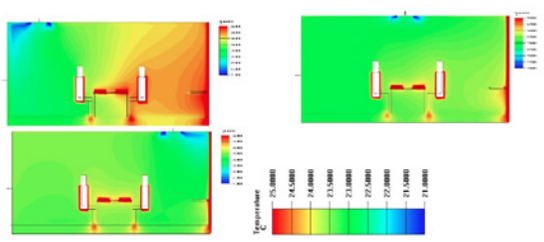

Figure 8: Temperature contours for an outdoor external temperature of 35°C, realized on plane 2 with varying positions of the chilled beam away from the external window (top left), middle of the room (top right), and next to the external window (bottom left); temperature legend is shown at the bottom.

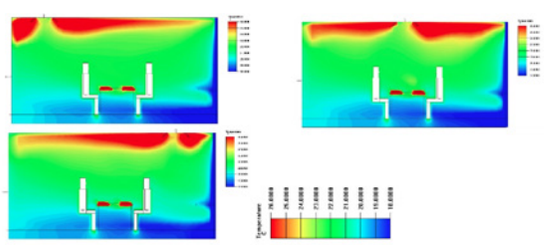

Figure 9: Temperature contours for an outdoor external temperature of -10°C, realized on plane 1 with varying positions of the chilled beam away from the external window (top left), middle of the room (top right), and next to the external window (bottom left); temperature legend is shown at the bottom.

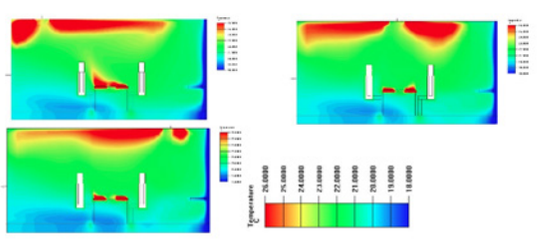

Figure 10: Temperature contours for an outdoor external temperature of -10°C, realized on plane 2 with varying positions of the chilled beam away from the external window (top left), middle of the room (top right), and next to the external window (bottom left); temperature legend is shown at the bottom.

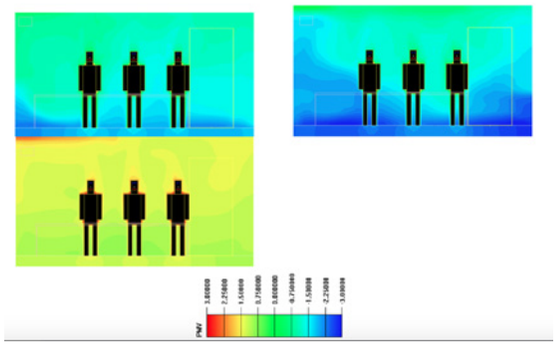

Figure 11: PMV realized on a plane perpendicular to both planes 1 and 2, with the door kept closed during April (top left), January (top right), and June (bottom left); PMV legend shown at the bottom.

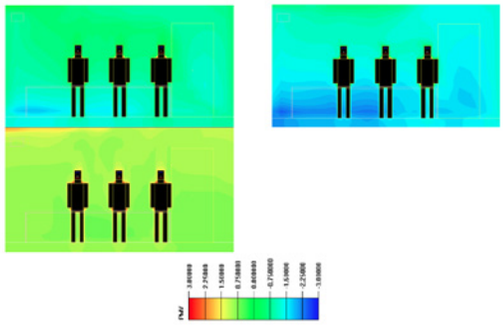

Figure 12: PMV realized on a plane perpendicular to both planes 1 and 2, with the door kept open during April (top left), January (top right), and June (bottom left); PMV legend shown at the bottom.

Figures 9 and 10 show the temperature distribution on planes 1 and 2 respectively with different locations of the chilled beam for an outdoor ambient temperature of -10°C. This is on average the lower end of the temperature conditions for a place like Andover, Massachusetts. The temperature of the incoming air into the test room from the chilled beam is 30°C. As in the case of higher external temperature, a slight moderation of the indoor conditions can be observed with the chilled beam being located close to the external window. The effect of the vertical stratification becomes prominent here, with the temperature difference between the ceiling and the floor being almost close to 8°C. One of the primary reasons for this is the arrangement of the furniture in the room—the two tables, one next to the window and another in the middle of the room. The air underneath the central table has minimal vertical circulation and the cold air flow along the external window is directed there by the near window table, making it colder than the average room temperature. This has an impact on the thermal comfort of the people, with the air temperature having a vertical gradient of almost 3°C from head to toe. In contrast to the heating scenario in winter, the cooling scenario has a significant difference in the temperature distribution between the two planes under consideration. This is also an outcome of having the near window table right next to the external window, along which the cold air from the chilled beam drops.

Similar simulations were also performed with two additional people added to the room to test the influence of the door being open versus closed. Figures 11 and 12 show the variation of Predictive Mean Vote (PMV) on a plane perpendicular to planes 1 and 2 described above but cutting across the people sitting at the table right by the door. Seasonal variations were also studied to assess the impact of door position on the comfort levels of people. For the purpose of comparison, air velocity and air change rate (ACH) values were assumed to be the same for the cases of the door open and closed.

It is observed that when the door is kept open, there is a better uniformity of temperature distribution within the room leading to relatively more comfortable PMV values. In addition to that, there would also be a draft flow of air from outside the room through the door, resulting in moderating the indoor conditions better and thereby influencing the PMV values. This is especially the case during the summer and shoulder seasons. During winter, the impact of the chilled beam flows is very minimal on the conditions close to the floor and hence the door position hardly plays any role in the comfort values. Another crucial observation from all these simulations and experiments is that the air temperature recorded near the thermostat controlling the room conditioning is found to be varying from the air temperature near the humans by around 1.5–3°C. Such a non-uniform distribution of temperature is found to be more impactful with an increasing number of people in the room.

Conclusions

A CFD model of a test room was simulated and validated using ANSYS and Airpak and a detailed analysis of the effect of the chilled beam location on the temperature and comfort conditions in the occupied space was conducted. In addition to the previously established facts of heat sources and large-scale circulations being the potential causes of the draft in the occupied space, it is also understood from this study that the opening of a door plays a major role in the air circulation within the space and can lead to potential drafts. However, this can help improve the air quality inside the conference room, as the human density is typically higher inside the conference room than outside. The direction of airflow through the door is dependent on multiple factors, primarily on the location of the chilled beam and the airflow rate through it, and this can be helpful in moderating the room conditioning. The location of the chilled beam in the room with respect to the distance from the external wall and window also plays an important role in counteracting the extreme outdoor weather conditions. Simulations analyzed in this work showed that the above-described effect is prominent when the chilled beam is located closer to the external windows and walls.

Acknowledgements

The authors would like to acknowledge Schneider Electric for providing the test room facility and other resources for conducting experiments to base the simulations on. This research was funded by Schneider Electric and Lenovo through the HKUST-MIT Research Alliance Consortium.

References

Fanger, P. O. (1970). Thermal comfort: Analysis and applications in environmental engineering. Danish Technical Press.

Koskela, H., Häggblom, H., Kosonen, R., & Ruponen, M. (2012). Flow pattern and thermal comfort in office environment with active chilled beams. *HVAC&R Research*, *18*(4), 723–736.

Muller, D., Gores, I., & Zielinski, R. (2004, September). Impact of the thermal load on the room airflow pattern. In *RoomVent 20014 9th International Conference on Air Distribution in Rooms* (pp. 5–8).

Nielsen, P. V., Allard, F., Awbi, H. B., Davidson, L., & Schälin, A. (2007). Computational Fluid Dynamics in Ventilation Design. *REHVA Guidebook No. 10*.

Zbořil, V., Melikov, A., Yordanova, B., Bozhkov, L., & Kosonen, R. (2007). Airflow distribution in rooms with active chilled beams. In *Proceedings of the 10th International Conference on Air Distribution in Rooms–Roomvent 2007* (pp. 1–7).